The Journal of Experimental Biology 208, 2753-2763
Published by The Company of Biologists 2005
doi:10.1242/jeb.01706



# Dorsal and anal fin function in bluegill sunfish *Lepomis macrochirus*: three-dimensional kinematics during propulsion and maneuvering

E. M. Standen* and G. V. Lauder

*Museum of Comparative Zoology, Harvard University, 26 Oxford Street, Cambridge, MA 02138, USA*

*Author for correspondence (e-mail: standen@fas.harvard.edu)

*Accepted 24 May 2005*

## Summary

**Dorsal and anal fins are median fins located above and below the centre of mass of fishes, each having a moment arm relative to the longitudinal axis. Understanding the kinematics of dorsal and anal fins may elucidate how these fins are used in concert to maintain and change fish body position and yet little is known about the functions of these fins. Using three synchronized high-speed cameras (500 frames $s^{-1}$) we studied the three-dimensional kinematics of dorsal and anal fins during steady swimming (0.5–2.5 *TL* $s^{-1}$, where *TL*=total length) and during slow speed maneuvers (0.5 *TL* $s^{-1}$). By digitizing points along every other fin ray in the soft-rayed portion of the fins we were able to determine not only the movement of the fin surface but also the curvature of individual fin rays and the resulting fin surface shape. We found that dorsal and anal fins begin oscillating, in phase, at steady swimming speeds above 1.0 *TL* $s^{-1}$ and that maximum lateral displacement of the trailing edge of the fins as well as fin area increase with increasing steady swimming speed. Differences in area, lateral displacement and moment arm between the dorsal and anal fin suggest that dorsal and anal fins produce balancing torques during steady swimming. During maneuvers, fin area is maximized and mean lateral excursion of both fins is greater than during steady swimming, with large variation among maneuvers. Fin surface shape changes dramatically during maneuvers. At any given point in time the spanwise (base to tip) curvature along fin rays can differ between adjacent rays, suggesting that fish have a high level of control over fin surface shape. Also, during maneuvers the whole surface of both dorsal and anal fins can be bent without individual fin rays exhibiting significant curvature.**

Key words: swimming, maneuvering, locomotion, dorsal fin, anal fin, kinematics, stability, bluegill sunfish, *Lepomis macrochirus.*

## Introduction

In 1926, when C. M. Breder published his classic monograph on the locomotion of fishes (Breder, 1926), little was known about how fish coordinate movement among fins. Despite Breder's wide-ranging functional and phylogenetic analysis of different modes of fish swimming, followed in 1930 by the pioneering physiological work of Eric von Holst (1973), who looked at general patterns of fish fin movement, our knowledge of coordinated fin function remains poor. Harris (1936, 1937), Breder and Edgerton (1942), Arreola and Westneat (1996), Gordon et al. (2000), Consi et al. (2001), Hove et al. (2001) and Liao (2002) have contributed important new data on multiple fin use during locomotion in fish, but in comparison to current understanding of body surface kinematics and hydrodynamics, quantitative information on how fish coordinate use among their fins is scant.

Fin use is an important issue for understanding fish locomotor biomechanics because fish are statically unstable (Eidietis et al., 2003; Harris, 1936, 1937; Webb, 2002, 2004b; Weihs, 1993). The size and position of fins relative to an animal's centre of mass (COM) will greatly affect how dynamic stability is achieved during locomotion. Perturbations in fish body position are caused by external environmental forces such as water currents, or by forces produced by their own fins, which may result in roll, pitch and yaw body movements (Fig. 1A). Fish use their fins to control body posture, and the relative position of fins to the centre of mass and centre of buoyancy (COB) is important in determining the forces and torques a fish experiences and produces during swimming. For example, Fig. 1B depicts dorsal and anal fin positions relative to the COM and COB of a typical fish. In this case, as is found in most fishes (Webb, 2004a,b), the COB is below the COM, causing rolling instability. The greater the distance of the fins from the midpoint between the COM and COB, the larger the moment arm for that fin. Assuming fins of similar size, one may predict that the anal fin in Fig. 1B would require less force to produce the same torque as the dorsal fin due to the length of its moment arm. Similarly, longitudinal and mediolateral position of fins on the fish's body will also affect pitch and yaw instabilities around the COM.

Webb (2002, 2004b) studied three species of fish with a diversity of fin morphologies and discovered that, for all species, postural disturbances that induced roll provoked the

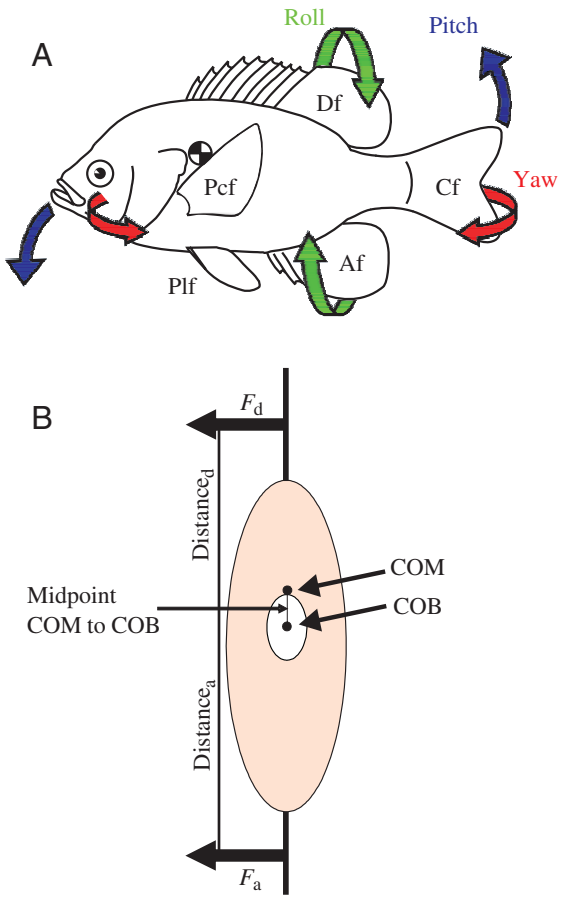


Fig. 1. (A) Fins and axes of instability in bluegill sunfish. Paired fins in bluegill are represented by the pectoral (Pcf) and pelvic fins (Plf). Dorsal (Df), anal (Af) and caudal (Cf) fins are median fins. Fins work to control the forces that act on the fish in three major axes; pitch (head up and down movement), roll (body rotating along its longitudinal axis) and yaw (head side to side movement). (B) Schematic cross-section showing centre of mass (COM), centre of buoyancy (COB) and fin placement. The white oval in the centre of the fish represents the swim bladder cavity of the animal. The area of the fin surface as well as its location relative to the fish's centre of mass and centre of buoyancy will determine the amount of torque a fin can impose on the body at a given velocity. Distance of the dorsal fin (Distance$_d$) and anal fin (Distance$_a$) are marked from the midpoint between the COM and COB. $F_d$, dorsal fin force; $F_a$, anal fin force.

fastest and most consistent recovery reaction, whereas yawing and pitching disturbances often elicited no response. The strong reaction of fish to correct for roll perturbations suggests important stabilizing functions for fins having the greatest ability to influence roll in fish: the dorsal and anal median fins.

Lauder and Drucker (2004) discuss the active role of dorsal fins during propulsion and maneuvering, as well as the absence of equivalent information available on the role of anal fins. Dorsal fin musculature is active during steady swimming and maneuvers, which suggests the soft-rayed portion of the fin acts as a control surface independent of the body (Jayne et al., 1996). Hydrodynamic studies of soft dorsal fins show that they produce lateral and posterolateral jets during swimming, suggesting that dorsal fins produce significant locomotory forces (Drucker and Lauder, 2001a,b). In many actinopterygian fishes the dorsal fin is often divided into two parts, spiny and soft-rayed portions. The anterior spiny dorsal fin in bluegill sunfish does not oscillate laterally during locomotion and is depressed during higher speed swimming. These observations suggest that the soft-rayed portion of the dorsal fin is responsible for the hydrodynamic forces recorded by Drucker and Lauder (2001a,b). Also, due to the relative position of fish fins, we hypothesize that soft dorsal fin hydrodynamic forces are, in large part, balanced by corresponding movements of the anal fin.

Currently no studies address the hypothesis that anal fin movement balances forces produced by dorsal fin motion. A quantitative three-dimensional kinematic analysis of anal fins simultaneous with dorsal fins is important to understand the existing dorsal fin hydrodynamic data. Subtleties in fin movement are determined by fin shape; therefore, the movement and positions of individual fin rays should also be studied because rays represent the fundamental mechanical support within fish fins. Fin rays appear to be intricately involved in fin surface control, but the motions of individual fin rays have not been quantified previously during fin movement in fishes.

In this paper, we present a three-dimensional kinematic analysis of the function of dorsal and anal fins during locomotion. We used three calibrated and synchronized video cameras to capture the three-dimensional movement of both dorsal and anal fins in bluegill sunfish *Lepomis macrochirus* Rafinesque 1819 during locomotion. We quantify dorsal and anal fin excursions, curvature of individual fin rays, and phase lags between fins during both steady and unsteady locomotion. Our goal is to use these kinematic data to describe patterns of coordinated movement between the dorsal and anal fins, compare and contrast fin ray motion within and between the two fins, and formulate hypotheses of anal fin hydrodynamic function for comparison to previous dorsal fin data.

## Materials and methods

### *Fish*

We collected data using six bluegill sunfish *Lepomis macrochirus* Rafinesque 1819 and analyzed in detail the four animals that had the most complete data sets. Fish were maintained in the laboratory, each in a separate 40 liter aquarium, and kept under a 12 h:12 h L:D photoperiod with a mean water temperature of 20°C (±1°C). The four individuals analyzed in this study had a mean total length (*TL*) of 16.25 cm (range 16–17 cm; S.E.M.=0.25).

### *Behavioral observations*

Bluegill swam in the centre of the working area (28 cm wide, 28 cm deep, 80 cm long) of a variable speed flow tank under conditions similar to those described in previous kinematic work on both *Lepomis* and *Oncorhynchus* (Drucker and Lauder,

2001a, 2003). Steady linear swimming was elicited from bluegill swimming at five speeds: 0.5 *TL* $s^{-1}$, 1.0 *TL* $s^{-1}$, 1.5 *TL* $s^{-1}$, 2.0 *TL* $s^{-1}$ and 2.5 *TL* $s^{-1}$. Fish also performed yawing turns while swimming at 0.5 *TL* $s^{-1}$. As in previous research (Drucker and Lauder, 2001b), turns were elicited using visual stimulus: a small-diameter wooden dowel was dropped into the tank along the flow tank wall lateral to the fish's head. The swimming behaviours induced in this study are directly comparable to those studied on the same species in the hydrodynamic analysis of Drucker and Lauder (2001a,b). To characterize the simultaneous movement of dorsal and anal fins during all behaviours we filmed fish using three synchronized high-speed video cameras (Photron Fastcam 1280×1024 pixels, HiDCam II 1280×1024 pixels, and a Photron APX system, 1024×1024 pixels) operating at 500 frames $s^{-1}$ (1/500 s shutter speed). The three camera system gave us a clear view of the dorsal fin, the anal fin and the lateral view of both fins, enabling us to make a simultaneous comparison of dorsal and anal fin kinematics (Fig. 2A).

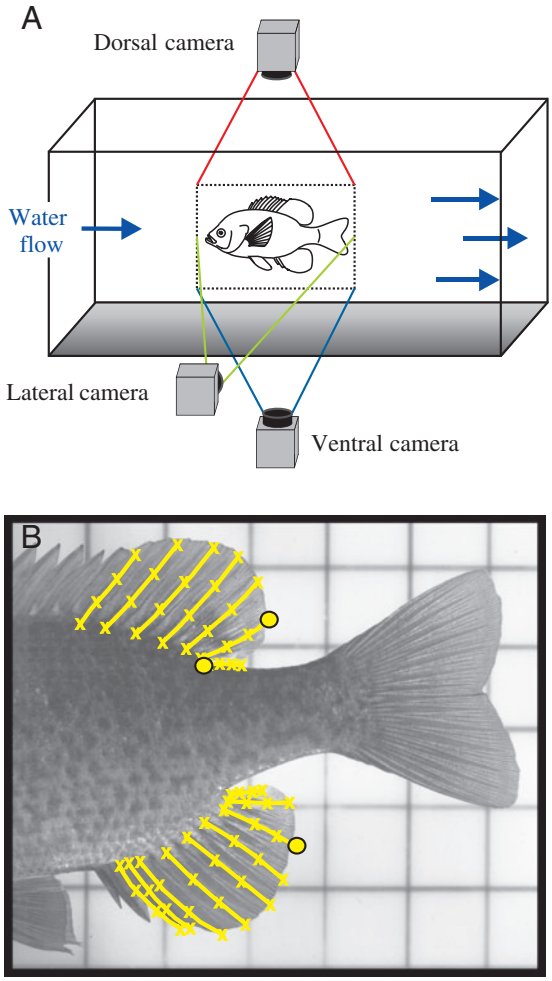


Fig. 2. Experimental apparatus. (A) Fish swam in a multi-speed flow tank. Three high-speed digital cameras captured synchronous dorsal, ventral and lateral views of swimming fish. (B) Fin ray digitizing. Four points along every other fin ray, represented here as yellow (x) symbols and lines, were digitized in three dimensions using two simultaneous views (only the lateral view is shown here) to calculate fin area and fin ray curvature. Yellow dots represent the trailing edge of each fin as well as the body point that were digitized to calculate excursion and phase lag.

### *Camera calibration*

To quantify the simultaneous spatial and temporal kinematics of the dorsal and anal fin, video sequences were analyzed using a custom digitizing program written using Matlab (version 6.5.1, Mathworks, Natick, MA, USA). The three temporally synchronized camera images were calibrated to view the same three-dimensional volume using a three-step process, detailed below.

First, a calibration cube with known location points was used to image the field of view of each pair of cameras: once for the dorsal–lateral camera pair and again for the ventral–lateral camera pair (Hsieh, 2003). These two separate calibration images were necessary because the dorsal and ventral cameras were located directly above one another (Fig. 2A) and therefore saw opposite sides of the calibration cube. To share enough points with the lateral view the calibration cube was rotated to face the dorsal–lateral camera pair and then the ventral–lateral camera pair, resulting in two separate calibration images. For each camera pair, the calibration cube filled the entire field of view in the *X*, *Y* and *Z* directions, and had no less than 23 points visible in both camera views simultaneously.

Second, a direct linear transformation (DLT) algorithm (Reinschmidt and van den Bogert, 1997) implemented in Matlab used the above calibration images to calculate and quantify the volume of the field of view for each of the camera pairs (dorsal–lateral and ventral–lateral). The DLT method uses 11 calculated coefficients to determine the positions of the cameras relative to each other and to a calibration coordinate system (our calibration cube). This removes linear image distortion. The calibration coordinate system must have a minimum of 15 non-coplanar points that maximally fill the field of view of the cameras to work successfully (Reinschmidt and van den Bogert, 1997). This volume calibration allowed accurate calculation of real world coordinates for any point digitized in both cameras of a given pair.

Third, to compare the dorsal–lateral image with the ventral–lateral image in three-dimensional space, we had to ensure that both volumes created by the DLT method had the same origin and three-dimensional coordinate axes. To do this we used a separate image with points of known location where a minimum of five points were visible in all three camera images (dorsal, ventral and lateral cameras). This image allowed us to apply a custom Matlab matrix rotation and translation program to align the dorsal–lateral volume and the ventral–lateral volume to the same three-dimensional coordinate axes.

### *Kinematic measurements*

A total of 112 swimming events performed by six fish were reviewed to establish general patterns of fin movement.

Detailed kinematic analysis was restricted to videos sampled from four fish during periods when they swam at constant speeds ($N$=11–13 fin beats per behaviour) or during turning maneuvers ($N$=7). Each sequence contained, at minimum, three consecutive tail-beats, and 20 points equally spaced in time per tail-beat were digitized. Kinematic analysis was completed on the portions of the fins that were actively moving during locomotion. The stiff, non-oscillating spiny portion of the fins was not included in the analysis. Although the spiny portions of the median fins may provide resistance to rolling caused by imbalance in the fishes body position, it appears that the role it plays in producing lateral forces that may be counteracted by the anal fin are negligible, particularly when considering the depression of the fin at higher speeds.

Calibration and fish images were digitized using a custom Matlab program. When a point was digitized in one camera image the DLT calibration coefficients were used to calculate a line in the second, corresponding image, along which this point could lie. This reference line, in combination with the second image, allowed precise location and digitization of a desired object in both images, and reduced digitizing error.

Excursion of dorsal and anal fins (mm) was calculated by digitizing the tip of the fin ray at the trailing edge of each fin. Body excursion (mm) was calculated by digitizing the posterior attachment point of the dorsal fin to the body (Fig. 2B). Observed phase lag (% of cycle) was calculated by analyzing excursion over time, and is the temporal difference in oscillation between the dorsal and anal fin and between each fin and the body. Expected phase lag (% of cycle) was calculated assuming the fins track the body, by measuring the longitudinal distance between the points used to depict the fins and body and representing these distances as a percent of the full oscillation cycle. Curvature (1/mm) and fin area ($mm^2$) were calculated when the posterior edge of each fin was at the point of greatest lateral excursion. Four evenly spaced points along every other fin ray were digitized to capture fin ray curvature and fin surface area (Fig. 2B). The equation of the line that describes the arc of the fin ray was calculated using a cubic spline in Matlab. The spanwise curvature at 20 points equally spaced along the fin ray line was calculated using the equation:

$$\kappa(s) = d\check{T} / ds ,$$

where $\kappa$ is curvature, $\check{T}$ is the tangent vector to the line and $s$ is the arc length along the line. To avoid emphasizing outlier data, maximum curvature was calculated by averaging the three highest curvature values of the 20 points calculated along each fin ray. The fin ray with the maximum value was then used to represent the maximum curvature of the fin in general. Fin area was estimated by summing the area of a triangular mesh generated from the 20 points per ray at which the curvature was calculated. Fin ray curvatures and area reported here are thus true three-dimensional curvatures and areas, not two-dimensional projected planar values.

Centre of mass was calculated by hanging preserved individuals on a string, first by a point posteriorly located on the dorsal side and again from a point anteriorly on the dorsal side. By superimposing the image of one fish exactly overtop of the other, the point at which the two lines of string would intersect represents the COM. Calculating the dorsoventral COM location for a series of fish allow estimation of the COM of the study individuals. Rolling axis was drawn on images of the study species as the horizontal axis, which ran longitudinally through the COM. Moment arm for each fin was

Table 1. *ANOVA for maximum fin and body excursion during steady swimming and maneuvers of bluegill sunfish*

| Source | d.f. | Type IV SS | Mean square | $F$-value | $P>F$ |
|---|---|---|---|---|---|
| Speed | 5 | 1338.16 | 267.63 | 41.84 | <0.0001 |
| Fish | 3 | 70.54 | 23.51 | 10.71 | <0.0001 |
| Speed × fish | 13 | 83.16 | 6.40 | 2.91 | 0.0007 |
| Fin | 2 | 270.73 | 135.36 | 70.91 | <0.0001 |
| Fish × fin | 6 | 11.45 | 1.91 | 0.87 | 0.5186 |
| Speed × fin | 10 | 163.80 | 16.38 | 11.74 | <0.0001 |
| Speed × fish × fin | 26 | 36.28 | 1.40 | 0.64 | 0.9138 |
| Residual | 180 | 395.25 | 2.20 | | |

Speed, fixed effect including all steady speeds and maneuvers; fish, random effect; fin, fixed effect including dorsal fin trailing edge, anal fin trailing edge and body where posterior dorsal fin meets body.
d.f., degrees of freedom; SS, sum of squares.

Table 2. *ANOVA for fin area at the point of maximum excursion during steady swimming and maneuvers of bluegill sunfish*

| Source | d.f. | Type IV SS | Mean square | $F$-value | $P>F$ |
|---|---|---|---|---|---|
| Speed | 5 | 850 665.32 | 170 133.06 | 16.33 | <0.0001 |
| Fin | 1 | 55 335.57 | 55 335.57 | 5.31 | 0.0278 |
| Speed × fin | 5 | 11 867.15 | 2373.43 | 0.23 | 0.9477 |
| Residual | 32 | 333 355.06 | 10 417.35 | | |

Speed, fixed effect including all steady speeds and maneuvers; fin, fixed effect including dorsal fin and anal fin; fish is excluded from the analysis due to limited degrees of freedom (d.f.).
SS, sum of squares.

Table 3. *ANOVA for maximum curvature of fin rays during steady swimming and maneuvers of bluegill sunfish*

| Source | d.f. | Type IV SS | Mean square | $F$-value | $P>F$ |
|---|---|---|---|---|---|
| Speed | 5 | 3.58302214 | 0.71660443 | 3.58 | 0.0111 |
| Fin | 1 | 0.02289706 | 0.02289706 | 0.11 | 0.7375 |
| Speed × fin | 5 | 0.25488856 | 0.05097771 | 0.25 | 0.9344 |
| Residual | 32 | 6.40739565 | 0.20023111 | | |

Speed, fixed effect including all steady speeds and maneuvers; fin, fixed effect including dorsal fin and anal fin; fish is excluded from the analysis due to limited degrees of freedom; curvature data is log transformed.
d.f., degrees of freedom; SS, sum of squares.

the distance from rolling axis to the anterior/posterior midpoint of the fin base.

### *Statistics*

Maximum fin excursion was analyzed using a three-way ANOVA with steady swimming speed and fin as fixed effects and fish as a random effect (Table 1). Area and maximum curvature of the fin were analyzed using two-way ANOVAs with swimming speed and fin as fixed effects, ensuring enough degrees of freedom (d.f.) to test the entire model (Quinn and Keough, 2002; Zar, 1999) (Tables 2, 3). Maximum curvature was log-transformed to normalize the data. Multiple comparisons within effects were made using least-square means (LSM) with a Bonferroni correction. Where missing values prohibited the use of LSM as a multiple comparison, individual *t*-tests were used and are noted as such in the results to enable conservative interpretation. For steady swimming speeds, during which the fish exhibited regular oscillatory swimming, expected phase lag due to fin and body position differences was compared with observed phase lag using three *t*-tests (Dorsal–Body, Dorsal–Anal and Anal–Body comparisons). *P*-values of the *t*-test were subject to Bonferroni correction. Significance levels for all tests were based on initial *P*-values of <0.05 and all statistical tests were completed using SAS (version 9.1 TS Level 1M2 XP_Pro Platform). Measurements noted in the text are expressed as mean ± S.E.M.

## Results

### *Whole fin kinematics*

While swimming steadily at 0.5 and 1.0 *TL* $s^{-1}$, bluegill use their pectoral fins only. Dorsal and anal fins remain motionless or have small, non-oscillatory movements (Fig. 3A,B). One fish did show some oscillatory movement of both dorsal and anal fins at all swimming speeds; however, at the lowest swimming speed of 0.5 *TL* $s^{-1}$ the dorsal and anal fin oscillations were not synchronized or consistent.

At speeds near or above 1.5 *TL* $s^{-1}$ bluegill begin swimming by oscillating their bodies and concurrently, their median fins. Dorsal and anal fin movement is regular and oscillatory (Fig. 3C–E). Maximum excursion differs significantly among speeds and between fins (Table 1, ANOVA, $N$=246, $P$<0.0001 for both variables; the fins variable includes three levels, dorsal fin trailing edge, anal fin trailing edge and body). Maximum excursion increases with steady swimming speed (Table 1, Fig. 4), overall, dorsal fins have larger excursions than anal fins (*t*-test, $N$=76, $P$<0.001), which have larger excursions than the body (*t*-test, $N$=76, $P$<0.001; Fig. 4). The phase shift between dorsal and anal fins that is observed in Fig. 3 is what would be expected as a result of the differences between longitudinal location of the digitized points on the trailing edges of the fins relative to each other along the body (observed phase-lag to expected phase-lag *t*-test, $N$=7, $P$=0.2691). The observed phase lag between anal fin and body and dorsal fin and body are significantly different from what would be expected (*t*-test,

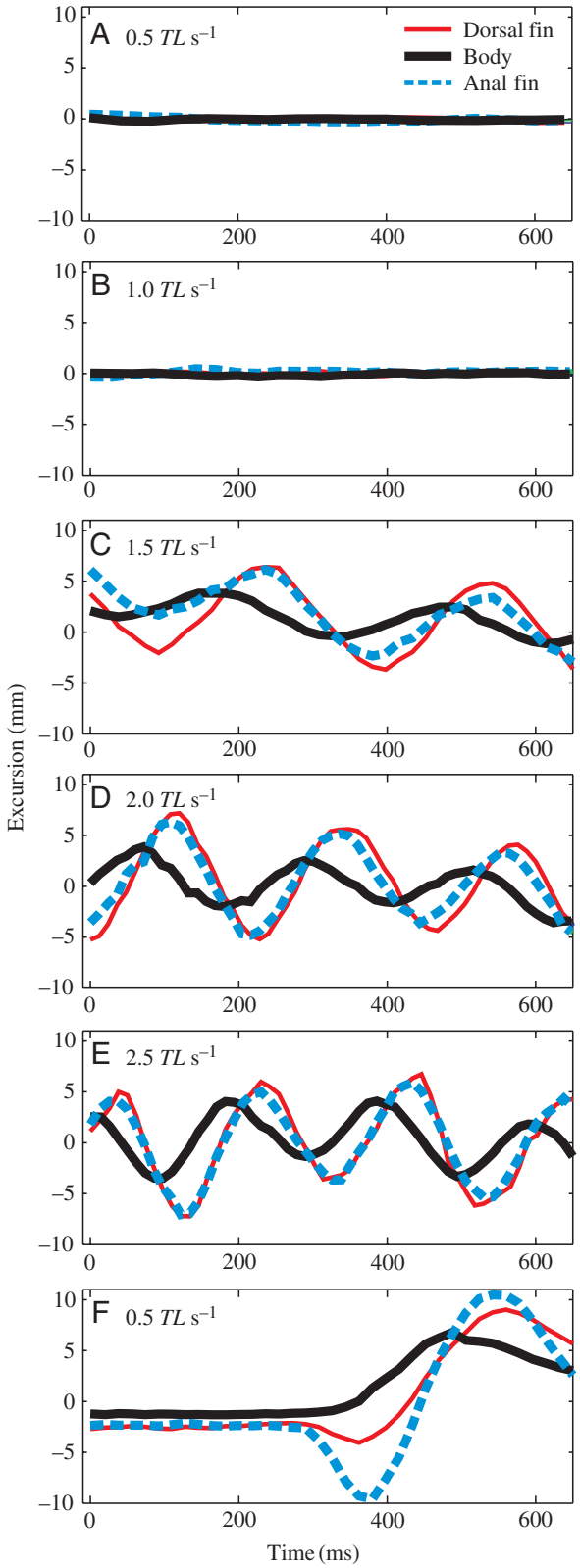


Fig. 3. (A–F) Plots of fin excursion over time; typical of steady swimming (A-E) and maneuvering (F) in bluegill. All graphs portray the same fish swimming at the five steady swimming speeds and during a maneuver. The black line represents the excursion of the body, the solid red line represents the dorsal fin, and the broken blue line represents the anal fin.

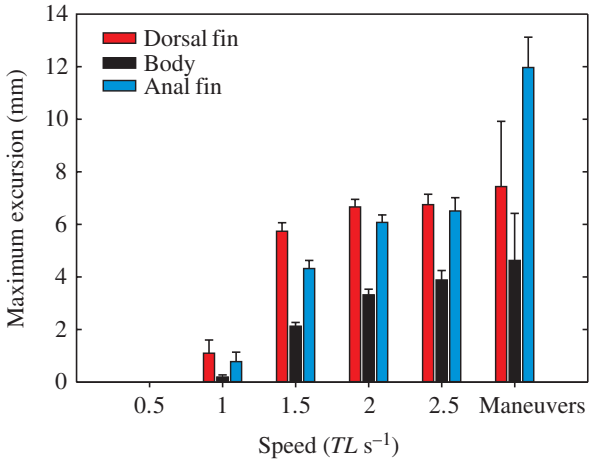


Fig. 4. Mean maximum excursion *vs* swimming speed. Maximum excursion increases with swimming speed. During steady swimming the dorsal fin (red) has larger excursions than the anal fin (blue) and both fins have greater excursions than the body (black). Unsteady maneuvers have highest maximum excursions and variation. Values are means ± 1 S.E.M. of all fish ($N$=4).

$N$=7, $P$=0.003 and $P$=0.000 respectively). There is no clear pattern to these phase shifts.

Both dorsal and anal fins are used during maneuvers but their motions become far more variable than during steady swimming. Both median fins move to the same side of the fish during maneuvers, and the excursion of the trailing edge of the fins can be greater than that of steady swimming (Figs 3F, 4, 5). On average maximum excursion of the anal fin during maneuvers is greater than that of the dorsal fin ($t$-test, $N$=6, $P$=0.058; Fig. 4). Kinematic variation is large during maneuvers. Fig. 5 shows the dorsal and anal fin positions at the point of maximum excursion during a maneuver. The large displacement of the trailing edge of both fins is evident from the dorsal and ventral camera views; however, the lateral view shows that actual deformation of the dorsal fin exceeds that of the anal fin in this particular example.

At all speeds and maneuvers the area of the dorsal fin is greater than that of the anal fin (Table 2; ANOVA, $N$=44, $P$=0.028). The area of both fins decreases with increasing steady swimming speed (speeds 0.5–1.0 *TL* $s^{-1}$ > speeds 1.5–2.5 *TL* $s^{-1}$; LSM comparison, Bonferroni corrected, $P \leqslant 0.003$; Fig. 6). During maneuvers the surface area of the fin exposed to water is high even though the shape of the fin surface changes dramatically (maximal fin area is achieved at swimming speeds of 0.5 *TL* $s^{-1}$; area during maneuvers is not different from speed 0.5–1.0 *TL* $s^{-1}$, LSM comparison, Bonferroni corrected, $P$=1.000; Fig. 6).

### *Fin ray curvature and fin surface bending*

Spanwise curvature measures the curve of the ray from its base to its tip. Chordwise curvature is the curve of the fin surface perpendicular to the fin rays, and is referred to here as fin surface shape. Maximum spanwise curvature of the fin rays is not significantly different among steady swimming speeds

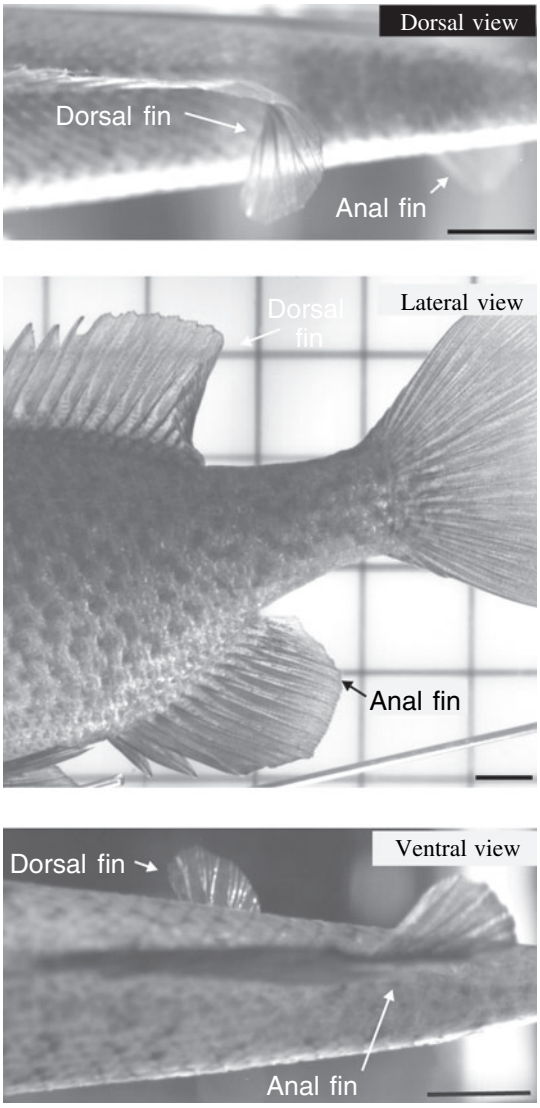


Fig. 5. Dorsal, lateral and ventral views of a yawing maneuver to the right at the point of maximum fin excursion. Both dorsal and anal fins show displacement of their trailing edges during this maneuver. Curvature of fin surfaces is large, but the actual bending of each individual fin ray is small. Note that both dorsal and anal fins move to the same side of the fish. Bars, 1 cm.

(Table 3; LSM comparison, Bonferroni, $N$=44, $P \geqslant 0.266$ for all comparisons). Fin ray curvature during maneuvers, however, is significantly greater than during slow steady swimming (0.5–1.0 *TL* $s^{-1}$; LSM comparison, Bonferroni corrected, $P \leqslant 0.041$ for all comparisons; Fig. 7). In both steady swimming and maneuvers, maximum curvature does not differ between dorsal and anal fins (ANOVA, $P$=0.738; Fig. 7). Curvature does differ, however, among individual fin rays within a single fin. For example, Fig. 8 shows curvature of individual fin rays at each swimming speed for both dorsal and anal fins. There appears to be no clear pattern of individual fin ray curvature along the length of the fin but there are clear differences in curvature of adjacent rays. This difference in

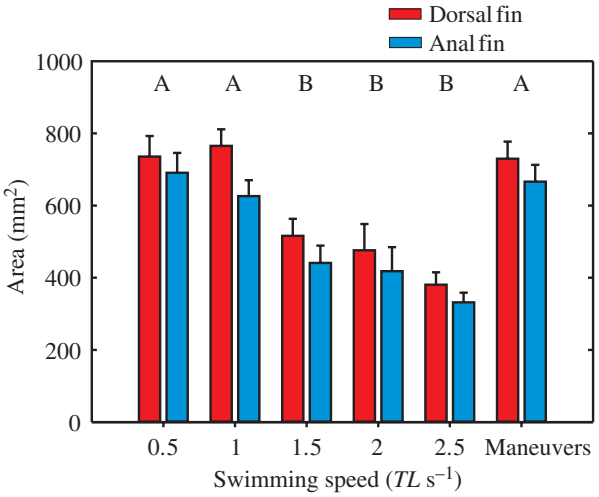


Fig. 6. Mean fin surface area at the time of maximum excursion. Fin area at swimming speeds denoted with letter A differ significantly from those denoted by letter B.

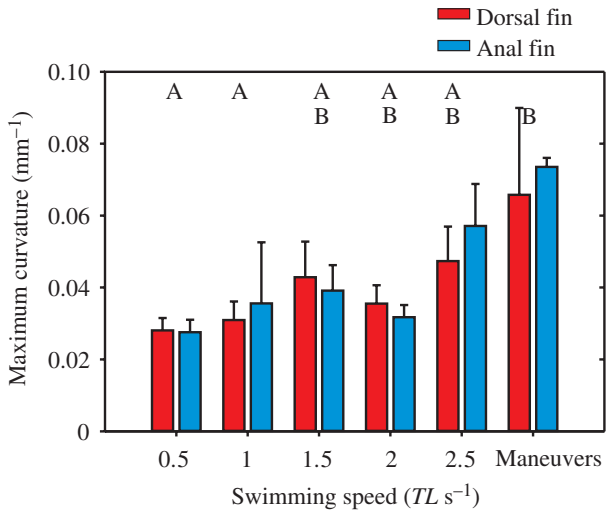


Fig. 7. Maximum curvature *vs* swimming speed. Maximum curvatures denoted with letter A differ significantly from those denoted by letter B.

curvature between adjacent fin rays suggests a high level of control over fin surface shape. During maneuvers the whole surface of both dorsal and anal fins can be bent without individual fin rays exhibiting significant curvature (Figs 5, 8). This suggests that individual rays are moving by rotation at the base of the ray, and that adjacent rays can be rotated varying amounts to achieve fin surface shape differences.

## Discussion

In this paper, we investigate the coordinated function of dorsal and anal fins during locomotion and the bending of individual fin rays within these fins. Studying fin movements during both steady swimming at multiple speeds and turning maneuvers reveals how fins interact to stabilize body position during locomotion. In addition to whole fin kinematics, we define changes in individual fin ray curvatures and ray position to describe patterns of three-dimensional fin shape change during locomotion.

### *Coordinated dorsal and anal fin function in bluegill sunfish*

Most studies involving the locomotory function of fish fins have focused on paired fins (Drucker and Jensen, 1996a,b; Drucker and Lauder, 2003), the caudal fin (Blake, 1983a; Lauder, 2000; Lauder et al., 2003) or represent theoretical, mathematical hypotheses of paired and median fin use (Blake, 1976, 1977, 1980, 1983b; Lighthill and Blake, 1990).

The few papers that have looked at dorsal and anal fins during locomotion focus on boxfish (ostraciiform swimmers with rigid trapezoid-shaped bodies) and burrfish (tetraodontiform swimmers; Arreola and Westneat, 1996; Gordon et al., 2000; Hove et al., 2001). These fishes are known to use their dorsal and anal fins differently in different gaits (Gordon et al., 2000; Hove et al., 2001). At swimming speeds below 1 *TL* s$^{-1}$ boxfish swim with a pectoral/anal fin dominant gait, where both pectoral and anal fins provide thrust for the animal and the dorsal fin is rarely used (Hove et al., 2001). At speeds above 1 *TL* s$^{-1}$ boxfish use dorsal/anal fin swimming, where synchronous oscillations of the dorsal and anal fin produce thrust and become the principle propulsors (Hove et al., 2001). Bluegill sunfish also exhibit different gaits while swimming but use their dorsal and anal fins only during body caudal fin steady swimming and during maneuvers. When swimming at speeds above 1.5 *TL* s$^{-1}$, bluegill sunfish use both dorsal and anal fins synchronously, with similar lateral excursions. Unlike the ostraciiform swimmers, there are no speeds at which bluegill use only the anal fin. At swimming speeds below 1.5 *TL* s$^{-1}$ most bluegill hold both dorsal and anal median fins motionless, and rely entirely on the pectoral fins and tail for propulsion.

When bluegill use their median fins for propulsion the dorsal and anal fins oscillate synchronously, showing no significant phase shift relative to each other (Table 1). The forces produced by fins and the symmetry of the fins in the sagittal plane of the animal may explain the synchronous movement of dorsal and anal fins. For example, the amount of torque a fin produces on the body of a fish depends on the moment arm of the fin (the distance the fin is from the COM), the surface area of the fin (how much water the fin is pushing) and fin velocity. Different methods can be used to calculate fin area, velocity, moment arm and resultant torque. Fins can be divided into strips, each having a moment arm, area, velocity and resultant torque. These values can be summed to calculate torque for the entire fin surface. This method provides good precision but, like all calculations, depends upon measurement accuracy to be useful. For the purposes of this study we do not divide the fins into strips to calculate torque; we use average fin areas, average velocity and a single moment arm for each fin. We do this because we are interested in the relative difference in torque production between the

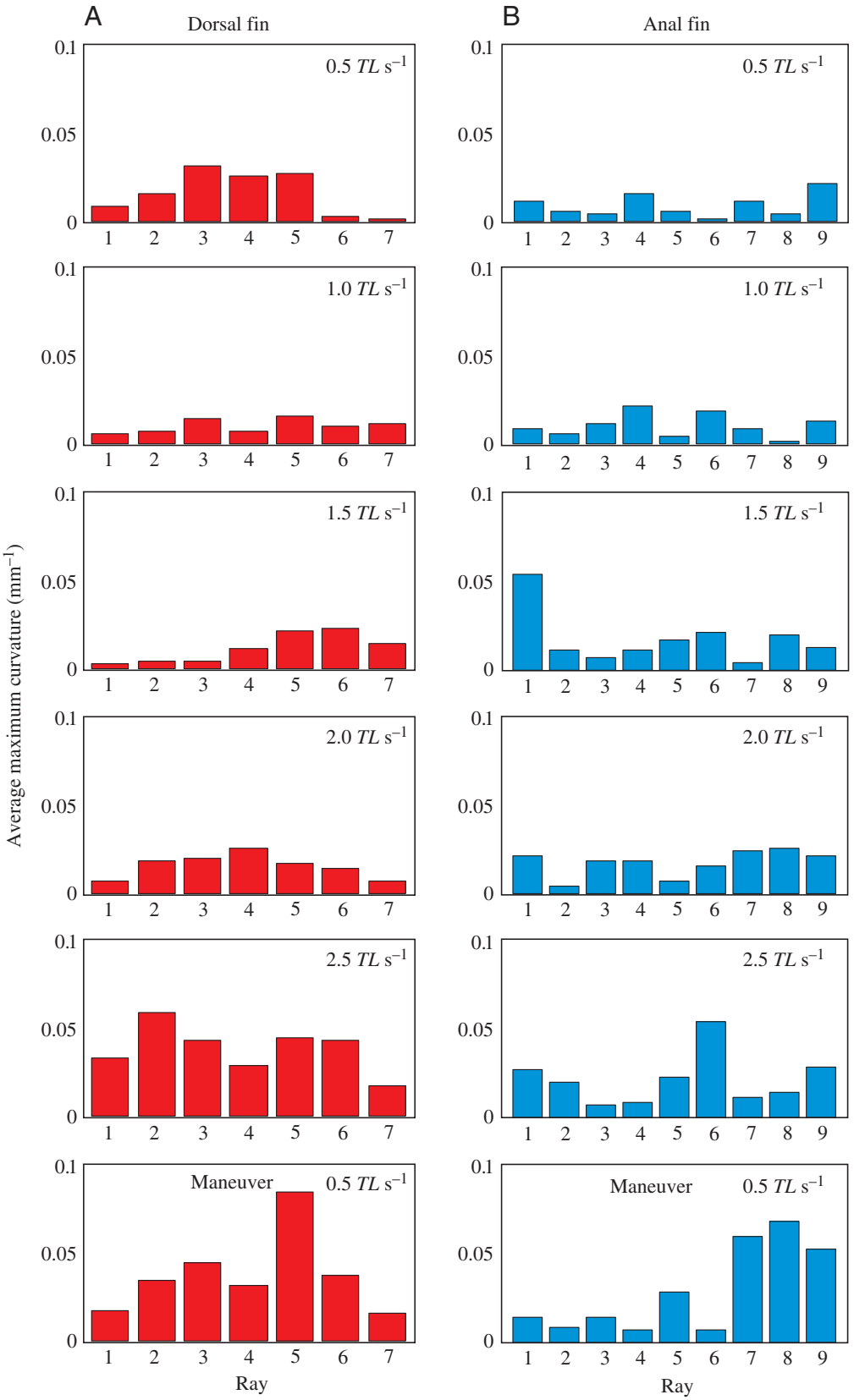


Fig. 8. Average maximum curvature of individual fin rays. Average maximum curvature was calculated as the average of the three maximum curvature values for each ray. Data are taken from a single fish. Individual rays are plotted on the *x*-axis with ray 1 being the most anterior along the fin; rays 2–7 are located posteriorly in order. Each graph represents a single swimming speed or maneuver at the point of maximum excursion. Seven rays were analyzed from the dorsal fin (A) and nine rays from the anal fin (B).

dorsal and anal fins and are limited by the accuracy with which the COM and fin moment arms can be calculated. Both the dorsal and anal fins attach to the body over a relatively broad area (about 1 cm), and the precise location where fin forces are transmitted to the body is not known. Using our method we find that although there are differences between dorsal and anal fins in the bluegill, the relative differences in moment arm (anal=23.7±0.65 mm, dorsal=21.4±0.48 mm), surface area (anal=529±32.09 $mm^2$, dorsal=601±34.79 $mm^2$) and excursion (steady swimming, anal=4.4±0.34 mm, dorsal=5.06±0.25 mm) between these fins suggests anal fins are producing similar torques on the body as those produced by dorsal fins. Fin forces that are synchronous and symmetrical will balance each other and create minimal net pitch, roll or yaw moments. Relative phases of dorsal and anal fin movement have been studied in needlefish, which have symmetric dorsal and anal fins, and needlefish show no phase lag between dorsal and anal fin oscillation (Liao, 2002).

Though dorsal and anal fins move together, oscillation of each fin relative to the body does show some phase shift. Both dorsal and anal fin oscillations vary inconsistently in timing from that of the body. The lack of phase matching between the dorsal and anal fins and the body suggests median fins have a more complex role than simply following the oscillation of the body during locomotion. The variation in timing of the anal fin also suggests it does more than balance the lateral thrust produced by the dorsal fin.

Both Harris (1936) and Breder (1926) suggest that the function of the anal fin is to act as a bilge keel (a high aspect ratio, rigid fin attached to the bottom or side of boats to attenuate rolling instabilities) straightening and balancing the body position of the animal as it produces forward thrust. Two major factors contribute to forces that cause possible perturbations for fish: the external environment and the fish's body and fin morphology. Environmental forces, such as turbulence, may not be predictable and, as long as they are the proper scale (Webb, in press), can perturb fish body position. Fish must react to these perturbations by using fins such as the anal fin to maintain an effective body position. The body shape and paired fin positioning of bluegill may also produce destabilizing forces, which must be balanced by the anal fin. Although the median fins and body shape of bluegill are relatively symmetrical around the long axis of the fish, the ventral paired pelvic fins make the fish dorso-ventrally asymmetrical, as there are no comparable fins on the dorsal edge of the body. The phase lag between anal fin and body may be the result of the anal fin acting not just as an oscillating foil to compliment the movement of the dorsal fin, but as a complex flexible foil, not a bilge keel, which provides a variety of movements required to stabilize the fish's body by counteracting forces encountered due to environmental turbulence and pelvic fin asymmetry.

### *Implications for stability*

Studying the kinematic performance of dorsal and anal fins allows one to make inferences about force production by these fins. Hydrodynamic studies using bluegill have shown that dorsal fins produce lateral jets of fluid during oscillation (Drucker and Lauder, 2001a,b; Lauder and Drucker, 2004). Because the kinematics of the anal fin are similar to those of the dorsal fin we hypothesize that the anal fin is also producing lateral fluid jets. Any jet produced lateral to the fish's longitudinal axis and above or below the COM will induce a rolling moment away from the direction of the jet (see roll, Fig. 1A). Dorsal and anal fins oscillate synchronously to the same side of the fish, one fin above the COM and one below at roughly the same longitudinal position on the fish. As a result, the lateral jets produced by each fin induce roll in opposite directions, balancing their rolling torque. By producing two strong lateral forces to the same side of the fish one might expect a lateral shift in body position or yawing, but this is not seen in steady swimming. Experimental work using flow visualization has shown that the wake of the dorsal fin may add momentum to the caudal fin wake (Drucker and Lauder, 2001a), increasing thrust for the animal. The extent to which the lateral forces produced by both the dorsal and anal fin are incorporated into axial and caudal fin movement is unknown; further flow visualization experiments would clarify the validity of this hypothesis. Theoretical work has also suggested benefits of the dorsal and anal fin acting as a 'double-tail', the thrust produced by dorsal and anal fins being out of phase with that of the caudal fin to maximize uniform thrust during locomotion (Webb and Weihs, 1983; Weihs, 1973).

As speed increases we see a decrease in both dorsal and anal fin area. The reduction of fin surface area may let fish control the magnitude of lateral jet production, while reducing surface area drag, which can be costly at higher swimming speeds. The ability of the fish to change its fin area gives it control over the force each fin produces. Force, be it lift or drag, is proportional to the velocity of the fin squared ($F \propto U^2$). Therefore, as swimming speed increases, velocity of water moving over the fin (velocity of the fin relative to the water) increases and a smaller fin area can produce the same force with a given movement.

During maneuvers, dorsal and anal fin motion results in yawing of the body, suggesting the fins are producing a larger jet to the side away from the turn. These fin movements and the resulting changes in body position are consistent with the understanding that median fins are capable of producing torques, which cause moments of yaw and roll (Drucker and Lauder, 2001b; Webb, 2004a). How fish are moving dorsal and anal fins relative to each other to produce these forces is unknown at present. During steady swimming the dorsal fin has a larger surface area and produces a larger magnitude lateral excursion compared to the anal fin. If this difference equates to the dorsal fin producing larger lateral forces than the anal fin, why then is there no visible rolling? This may be because the rolling moment arm of the anal fin is longer than that of the dorsal fin (anal=23.7±0.65 mm, dorsal=21.4±0.48 mm; Fig. 1B). A fin with a longer moment arm requires less force to produce the same amount of torque, compared to a fin with a shorter moment arm. The slightly

longer moment arm found in the anal fin may explain why it generally shows smaller area and excursions in steady swimming than the dorsal fin (Figs 4, 5). The large amplitude motion of the anal fin during maneuvering suggests that the anal fin may be critical in initiating a large rolling moment, unbalanced by the dorsal fin, which leads into the visible lateral yawing of the fish's body, accompanied by some roll. Calculation of actual values for forces generated by dorsal and anal fins, and hence torques, awaits future flow visualization analysis.

### *Fin ray function*

Overall fin shape is the result of the position of individual fin rays. Fin rays show different curvatures from base to tip and different positions relative to their base depending on swimming speed and maneuver (Figs 7, 8). Curvature between adjacent fin rays can also be very different. A clear example of this can be seen in the dorsal fin plot of swimming speed 2.5 $TL\ s^{-1}$ in Fig. 8; rays 1, 2 and 3 all display different maximum curvatures, suggesting they have some independence from one another. The ability of fish to adjust the curvature of individual rays suggests a greater control over fin surface shape than if all rays were confined to the same curvature at a given point in time; fish fins can have different spanwise curvatures depending on the longitudinal position along the fin surface. In addition, the shape of the whole fin surface can be dramatically bent without extreme curvature of individual rays. This bending of the fin surface appears to be mostly achieved by a rotation of individual fin rays at their base. As can be seen in Fig. 5, both dorsal and anal fins are bent nearly 90°. Despite this large deformation of the fin surface, the individual rays are only modestly curved, as can be seen visually in Fig. 5. The position of the ray and its curvature appear to be independent control mechanisms, allowing the fish multiple degrees of freedom in fin ray and thus fin surface control. The diversity of possible curvatures within individual rays and the multitude of angles that a ray can occupy during a fin stroke allow considerable diversity of fin surface shape and position.

Ray curvature during maneuvers is larger relative to steady swimming (Fig. 7) but still remains small. Consider the units of curvature, $1/R$, where $R$ is the radius of the circle around which the fin ray would curve if it held that maximum curvature along its entire length. Because the length of the rays are generally <3 cm it would take a very small circle to produce a large curve in the ray. The maximum curvature measured during a maneuver is $<0.1\ mm^{-1}$, which corresponds to a circle with a radius of 10 mm and therefore a relatively modest curvature for a ray at its most curved point.

The curvature seen during maneuvers involving large whole fin surface displacements (see Fig. 5), may be due to a combination of fin ray mechanics and fluid pressure forces (normal to the fin) as the fin pushes against water. Each fin ray is composed of two hemitrichia (together termed a lepidotrich; Geerlink and Videler, 1987; Haas, 1962; Lanzing, 1976), and each hemitrich is made of a series of bony elements, which form a semi-circular rod-like structure. The hemitrichia are attached to one another along their concave sides by elastic fibers; these fibers allow the hemitrichia to slide slightly relative to one another. The base of each hemitrich is wide and supports a large area for the attachment of erector, depressor and inclinator muscles (Winterbottom, 1974), which permit rotation of each fin ray as well as motion of hemitrichia relative to each other.

Muscles that pull on one hemitrich while the other is held in position cause curvature of the whole fin ray (Geerlink and Videler, 1987). Hemitrichia are of fixed length and cannot shorten; if fin muscles pull on one hemitrich while the other remains anchored at its base, both hemitrichia slide and bend relative to each other, resulting in the curvature of the fin ray towards the direction of the pulled hemitrich (Geerlink and Videler, 1987). One might hypothesize that equal contraction of musculature attaching to both hemitrichia would not cause curvature. But, depending on the combination of muscles used, the entire fin ray may rotate around its base, changing the position of the entire ray without changing its curvature. Because ray position contributes to fin surface shape, this hypothesis would explain the ability of the fish to change the surface shape of fins without large curvature occurring in individual fin rays.

Fin ray curvature may also be reduced by normal pressures on the fin caused by water flow. For example, in Fig. 5, dorsal fin surface is deformed to lie 90° to the direction of the water flow. The normal pressure of the water on the surface of the fin may push with enough force to straighten rays that would otherwise curve forward into the flow.

The mechanisms of base rotation and fin ray curvature combined would allow fish to change the whole fin surface shape with far more control than if it had only one or the other mechanism. Confirming the hypothesis that fin ray base rotation and hemitrich sliding are the mechanisms that account for the observable fin surface control we see during locomotion will require measuring the activation patterns and force outputs of the muscles attached to the fin rays in future experiments.

We are grateful to all the people in the Lauder Laboratory, particularly Peter Madden who wrote the three-dimensional digitizing program and supplied much Matlab advice. Thanks also to Eric Tytell for Matlab assistance and, along with Jen Nauen, for thoughtful review comments. The fish in this project were well maintained by Jeremiah Alexander. Funding for this project was provided by NSF IBN0316675 to G.V.L.

## References

**Arreola, V. I. and Westneat, M. W.** (1996). Mechanics of propulsion by multiple fins: Kinematics of aquatic locomotion in the burrfish. *Proc. R. Soc. Lond. B* **263**, 1689-1696.

**Blake, R. W.** (1976). On seahorse locomotion. *J. Mar. Biol. Assn UK* **56**, 939-949.

**Blake, R. W.** (1977). On ostraciiform locomotion. *J. Mar. Biol. Assn UK* **57**, 1047-1055.

**Blake, R. W.** (1980). Undulatory median fin propulsion of two teleosts with different modes of life. *Can. J. Zool.* **58**, 2116-2119.

**Blake, R. W.** (1983a). Functional design and burst-and-coast swimming in fishes. *Can. J. Zool.* **61**, 2491-2494.

**Blake, R. W.** (1983b). Swimming in the electric eels and knifefishes. *Can. J. Zool.* **61**, 1432-1441.
**Breder, C. M.** (1926). The locomotion of fishes. *Zoologica-New York* **4**, 159-297.
**Breder, C. M. and Edgerton, H. E.** (1942). An analysis of the locomotion of the seahorse, *Hippocampus*, by means of high speed cinematography. *Ann. NY Acad. Sci.* **43**, 145-172.
**Consi, T. R., Seifert, P. A., Triantafyllou, M. S. and Edelman, E. R.** (2001). The dorsal fin engine of the seahorse (*Hippocampus* sp.). *J. Morphol.* **248**, 80-97.
**Drucker, E. G. and Jensen, J. S.** (1996a). Pectoral fin locomotion in the striped surfperch. 1. Kinematic effects of swimming speed and body size. *J. Exp. Biol.* **199**, 2235-2242.
**Drucker, E. G. and Jensen, J. S.** (1996b). Pectoral fin locomotion in the striped surfperch. 2. Scaling swimming kinematics and performance at a gait transition. *J. Exp. Biol.* **199**, 2243-2252.
**Drucker, E. G. and Lauder, G. V.** (2001a). Locomotor function of the dorsal fin in teleost fishes: experimental analysis of wake forces in sunfish. *J. Exp. Biol.* **204**, 2943-2958.
**Drucker, E. G. and Lauder, G. V.** (2001b). Wake dynamics and fluid forces of turning maneuvers in sunfish. *J. Exp. Biol.* **204**, 431-442.
**Drucker, E. G. and Lauder, G. V.** (2003). Function of pectoral fins in rainbow trout: behavioural repertoire and hydrodynamic forces. *J. Exp. Biol.* **206**, 813-826.
**Eidietis, L., Forrester, T. L. and Webb, P. W.** (2003). Relative abilities to correct rolling disturbances of three morphologically different fish. *Can. J. Zool.* **80**, 2156-2163.
**Geerlink, P. J. and Videler, J. J.** (1987). The relation between structure and bending properties of teleost fin rays. *Neth. J. Zool.* **37**, 59-80.
**Gordon, M. S., Hove, J. R., Webb, P. W. and Weihs, D.** (2000). Boxfishes as unusually well-controlled autonomous underwater vehicles. *Physiol. Biochem. Zool.* **73**, 663-671.
**Haas, H. J.** (1962). Studies on mechanisms of joint and bone formation in skeleton rays of fish fins. *Dev. Biol.* **5**, 1-34.
**Harris, J. E.** (1936). The role of the fins in the equilibrium of the swimming fish. I. Wind-tunnel tests on a model of *Mustelus canis* (Mitchill). *J. Exp. Biol.* **13**, 476-493.
**Harris, J. E.** (1937). The mechanical significance of the position and movements of the paired fins in the Teleostei. *Pap. Tortugas Lab.* **31**, 173-189.
**Hove, J. R., O'Bryan, L. M., Gordon, M. S., Webb, P. W. and Weihs, D.** (2001). Boxfishes (Teleostei: Ostraciidae) as a model system for fishes swimming with many fins: kinematics. *J. Exp. Biol.* **204**, 1459-1471.
**Hsieh, S. T.** (2003). Three-dimensional hindlimb kinematics of water running in the plumed basilisk lizard (*Basilisk plumifrons*). *J. Exp. Biol.* **206**, 4363-4377.
**Jayne, B. C., Lozada, A. F. and Lauder, G. V.** (1996). Function of the dorsal fin in bluegill sunfish: motor patterns during four distinct locomotor behaviours. *J. Morphol.* **228**, 307-326.
**Lanzing, W. J. R.** (1976). The fine structure of fins and finrays of *Tilapia mossambica* (Peters). *Cell Tissue Res.* **173**, 349-356.
**Lauder, G. V.** (2000). Function of the caudal fin during locomotion in fishes: kinematics, flow visualization, and evolutionary patterns. *Am. Zool.* **40**, 101-122.
**Lauder, G. V. and Drucker, E. G.** (2004). Morphology and experimental hydrodynamics of fish fin control surfaces. *IEEE J. Oceanic Eng.* **29**, 556-571.
**Lauder, G. V., Drucker, E. G., Nauen, J. C. and Wilga, C. D.** (2003). Experimental hydrodynamics and evolution: caudal fin locomotion in fishes. In *Vertebrate Biomechanics and Evolution* (ed. J.-P. G. Vincent, L. Bels and A. Casinos), pp. 117-135. Oxford: BIOS Scientific Publishers.
**Liao, J. C.** (2002). Swimming in needlefish (Belonidae): anguilliform locomotion with fins. *J. Exp. Biol.* **205**, 2875-2884.
**Lighthill, J. and Blake, R.** (1990). Biofluid dynamics of balistiform and gymnotiform locomotion. 1. Biological background, and analysis by elongated-body theory. *J. Fluid Mech.* **212**, 183-207.
**Quinn, G. P. and Keough, M. J.** (2002). *Experimental Design and Data Analysis for Biologists.* Cambridge, UK: Cambridge University Press.
**Reinschmidt, C. and van den Bogert, T.** (1997). *Kinemat: A MATLAB toolbox for three-dimensional kinematic analyses*. Calgary: Human Performance Laboratory: The University of Calgary.
**von Holst, E.** (1973). *The Behavioural Physiology of Animals and Man; the Collected Papers of Eric von Holst*. Coral Gables, FL: University of Miami Press.
**Webb, P. W.** (2002). Control of posture, depth, and swimming trajectories of fishes. *Integr. Comp. Biol.* **42**, 94-101.
**Webb, P. W.** (2004a). Maneuverability-General issues. *IEEE J. Oceanic Eng.* **29**, 547-555.
**Webb, P. W.** (2004b). Response latencies to postural disturbances in three species of teleostean fishes. *J. Exp. Biol.* **207**, 955-961.
**Webb, P. W.** (in press). Stability and maneuverability. In *Fish Biomechanics* (ed. R. E. Shadwick and G. V. Lauder). San Diego: Elsevier.
**Webb, P. W. and Weihs, D.** (1983). *Fish Biomechanics.* New York: Praeger.
**Weihs, D.** (1973). The mechanism of rapid starting in the slender fish. *Biorheology* **10**, 343-350.
**Weihs, D.** (1993). Stability of aquatic animal locomotion. *Cont. Math.* **141**, 443-461.
**Winterbottom, R.** (1974). Descriptive synonymy of striated muscles of Teleostei. *Proc. Acad. Nat. Sci. Phila.* **125**, 225-317.
**Zar, J. H.** (1999). *Biostatistical Analysis*. Upper Saddle River, New Jersey: Prentice Hall.